3 GERDA: Neutrinoless Double Beta Decay in Ge

Laura Baudis, Giovanni Benato, Andreas James, Alexander Kish,
Michael Miloradovic, Manuel Walter

in collaboration with: INFN Laboratori Nazionali del Gran Sasso LNGS, Jagellonian University Cracow, Institut für Kern- und Teilchenphysik Technische Universität Dresden, Joint Institute for Nuclear Research Dubna, Institute for Reference Materials and Measurements Geel, Max Planck Institut für Kernphysik Heidelberg, Universitá di Milano Bicocca e INFN Milano, Institute for Nuclear Research of the Russian Academy of Sciences, Institute for Theoretical and Experimental Physics Moscow, Russian Research Center Kurchatov Institute, Max-Planck-Institut für Physik München, Dipartimento di Fisica dell Universitá di Padova e INFN, Physikalisches Institut Eberhard Karls Universität Tübingen.

(GERDA Collaboration)

Neutrino oscillation experiments show that neutrinos mix so neutrino mass eigenstates differ from weak eigenstates, *i.e.* neutrinos have mass and the Standard Model (SM) must be extended to include the observed lepton flavor violation. One possibility is to allow left-handed neutrinos only so the mass eigenstates are Majorana fermions, and the 3×3 mixing matrix depends on six independent parameters, the three mixing angles and three physical phases. Meanwhile the magnitudes of all elements of the leptonic mixing matrix are determined [1].

While oscillation experiments provide information on the mass squared differences, and on the leptonic mixing angles, they are insensitive to the absolute mass scale of neutrinos. Such information can be extracted from kinematic studies of Tritium (and other) beta decays, and from the neutrinoless double beta decay ($0\nu\beta\beta$). More importantly this decay, if observed, would proof that the neutrino is a Majorana fermion and that total lepton number is not conserved in nature. The rate of the extremely rare nuclear process is proportional to the effective Majorana neutrino mass, $\langle m \rangle_{eff} = \Sigma_i U_{ei}^2 m_i$, where the sum is over the three generations and U_{ei}, the elements of the lepton mixing matrix, are complex numbers.

Limits on $\langle m \rangle_{eff}$ have been obtained for a variety of nuclei, see [2] for a recent review. The most stringent upper limit for ^{76}Ge comes from GERDA [3], as detailed below, while the best limits for ^{130}Te and ^{100}Mo, $\langle m \rangle_{eff} \leq 0.2 - 0.7\,\text{eV}$, and $\langle m \rangle_{eff} \leq 0.45 - 0.9\,\text{eV}$, respectively, come from the Cuoricino and NEMO-3 experiments. Recently, experiments using xenon in its liquid form, EXO, and mixed with a scintillator, KamLAND-ZEN, provided very competitive upper limits of $\sim 0.2 - 0.25\,\text{eV}$ and $\sim 0.2 - 0.5\,\text{eV}$, respectively.

3.1 The GERDA experiment

The GERDA experiment at LNGS searches for the $0\nu\beta\beta$-decay of ^{76}Ge. High-purity germanium (HPGe) detectors enriched in ^{76}Ge are operated bare, immersed in liquid argon (LAr). The argon is surrounded by a 3 m thick water Cherenkov shield. A clean room for Ge diode handling is installed on top of the water tank, with a lock at its center for transferring detectors into the Ar [4].

GERDA phase I took data at LNGS from 2011-2013 with about 18 kg of enriched HPGe detectors, accumulating an exposure of 21.6 kg·y. Pulse shape discrimination (PSD) is used to distinguish signal events which have primarily a single interaction site within the detector bulk from background events which are dominated by interactions on the surface or by multiple interactions. A flat background was predicted in the 1930 -2190 keV region of interest [5]. No events above background are observed in the resulting energy spectrum, shown in Fig. 3.1. The resulting lower limit (90% C.L.) on the half-life, 2.1×10^{25} y corresponds to an upper limit on the effective neutrino

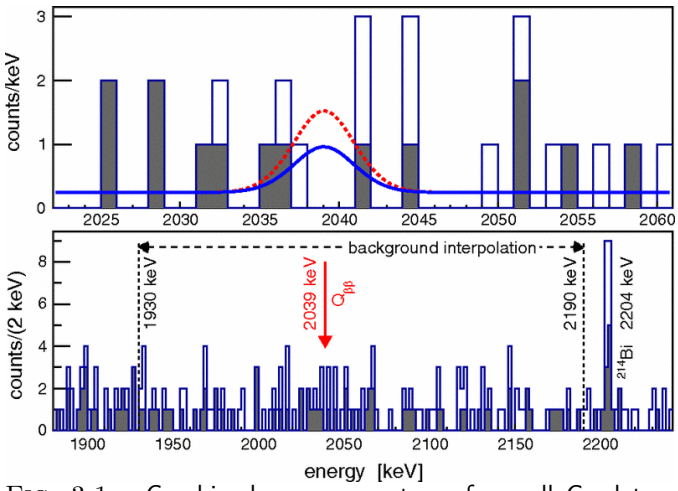

FIG. 3.1 – Combined energy spectrum from all Ge detectors without (with) PSD, indicated by the open (filled) histogram. A zoom around $Q_{\beta\beta}$ is shown in the upper panel, along with the expectation from $T_{1/2} = 1.19\times10^{25}$ y (red dashed) [6] and the the 90% upper limit $T_{1/2} < 2.1\times10^{25}$ y (blue solid) derived from this measurement.

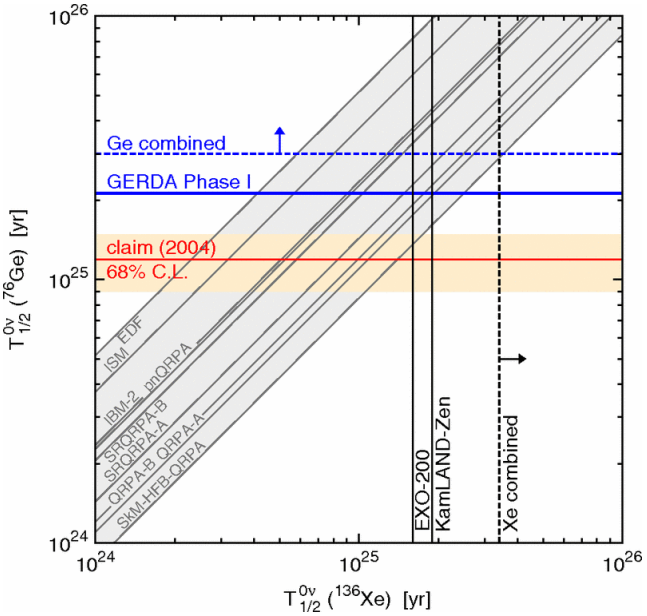

FIG. 3.2 – Limits (90% C.L.) on $T_{1/2}$ from ^{76}Ge and ^{136}Xe, compared with the signal claim for ^{76}Ge [6]. The lines in the shaded grey band are the predictions for the correlation of the half-lives according to different NME calculations. Figure from [3].

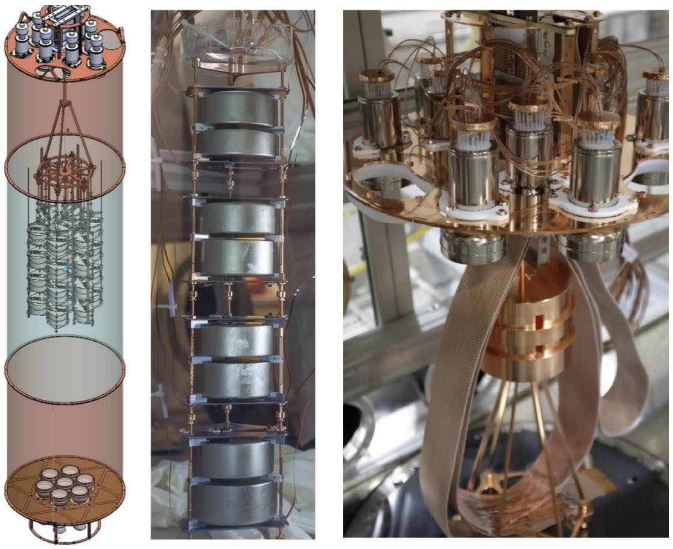

FIG. 3.3 – Left: Schematic view of the GERDA phase II Ge detector and LAr veto arrangement.
Centre: A string of eight BEGe detectors in GERDA phase II. These are grouped in pairs within one holder.
Right: Part of the phase II liquid argon veto during its installation at LNGS. The top PMT array (of Hamamatsu R11065, low-radioactivity type) can be clearly seen.

mass of $\langle m \rangle_{eff} \leq 0.2 - 0.4\,\text{eV}$, depending on the nuclear matrix element [3]. This result strongly challenges the claim of a signal by part of the Heidelberg-Moscow collaboration [6], as shown in Fig. 3.2. Recently, results on the decay with emission of Majorons were submitted for publication [7].

The second phase of the experiment aims at a total exposure of 100 kg·y with a background around $Q_{\beta\beta}$ reduced by a factor ten to 10^{-3} counts/(keV·kg·y). The half-life sensitivity is 2×10^{26} y and the corresponding range of effective neutrino masses is $\leq 0.09 - 0.15$ eV, taking into account the uncertainty in the matrix element and neglecting new lepton number violating interactions.

All thirty (20.5 kg) enriched phase II detectors, of broad-energy germanium (BEGe) type, were produced, characterised [8] and are now under commissioning in the LAr cryostat at LNGS. Figure 3.3 shows a schematic view of the arrangement, and pictures of a BEGe detector string and the liquid argon veto. The latter will allow to reduce background events with depositions in both the LAr and a Ge detector (see below). We expect to start data taking in late summer 2015.

3.2 Analysis of calibration and physics measurements

We are strongly involved in the analysis of the GERDA calibration and physics data. During phase I the energy resolution suffered from low-frequency baseline fluctuations. A digital filter with enhanced low-frequency noise rejection was developed and tested as an alternative to the standard Gaussian shaping. It consists of a cusp filter with a central flat-top for maximizing the charge integration. The distortion induced by the preamplifier is removed via a deconvolution with the preamplifier response function. The effect of this Zero-Area finite-length Cusp filter (referred as *ZAC filter*) is illustrated in Figs. 3.4 and 3.5. The energy is estimated as the peak value of the shaped signal.

We have tuned the filter parameters for each detector separately, and all phase I data have been successfully reprocessed, leading to an average improvement of 0.3 keV at $Q_{\beta\beta}$ for the calibration data [9]. The impact on the physics reach of GERDA phase I is $\sim$ 5% in median sensitivity. The reprocessed phase I data will be combined with the new results from phase II.

Since the PSD performance is strongly affected by the noise conditions as well a noise-reduction algorithm was implemented which transforms the raw wavelet as shown in Fig.3.6). The algorithm can calculate a threshold based on the noise observed in each individual event. We will test this method on the current pulse instead of using the raw trace (charge pulse).

The larger number of Ge detectors and the longer duration of phase II make the use of a robust, fully automatized and well documented analysis software mandatory. In order to minimize the proliferation of single purpose

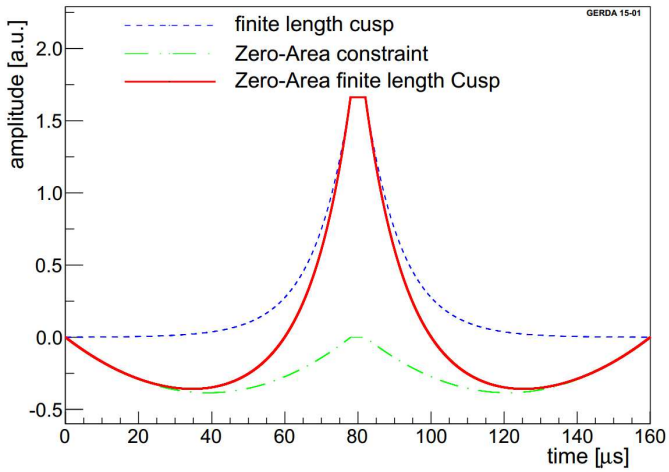

FIG. 3.4 – ZAC filter composed of the finite-length cusp from which two parabolas are subtracted on the sides.

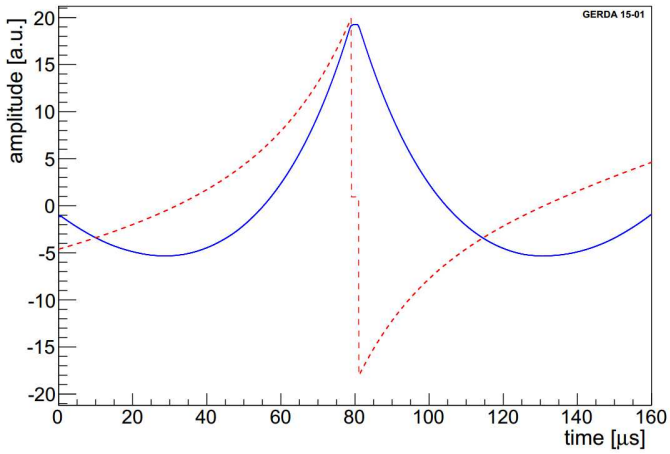

FIG. 3.5 – The ZAC filter after the de-convolution with the preamplifier response function (red) and the resulting waveform (blue).

software packages we are developping a multi-purpose software framework. Main tasks are the optimization of the filters for energy reconstruction and PSD discussed above, the event selection through dedicated quality cuts and the energy calibration. Tools are being developed to constantly monitor the noise conditions which will automatically tag data periods with stable noise features, for which a single filter can be employed. The software will be interfaced to a CouchDB database for the storage of the main output parameters, *e.g.* the quality cuts values, the calibration curves, as well as the PSD and LAr veto selections.

3.3 Production and characterization of the calibration sources for phase II

We are responsible for the calibration system hardware and software [10]. In preparation for the start of GERDA phase II we produced four low neutron emission ^{228}Th sources by depositing the radioactive material on high purity gold foils. The emitted neutron flux was measured with a ^{3}He counter and a low background LiI(Eu) detector, located underground at LNGS. As an example, Fig. 3.7 shows the spectrum recorded by our LiI(Eu) detector with the four phase II sources and background spectrum recorded during 142 days. These results proof for the first time that LiI(Eu) can detect very low neutron fluxes. The neutron rates measured with the LiI(Eu) and the ^{3}He detectors are 8.2 ± 2.3 n/s/Bq and 9.4 ± 2.3 n/s/Bq, respectively, which is an order of magnitude less than observed with standard ^{228}Th sources measured with the same procedure.

Moreover, this result confirms the reproducibility of our source production, developed for phase I. ^{228}Th sources with reduced neutron strength are of interest for other low background experiments too, when the activation of material close to the detector is of relevance.

The γ activity of each source was measured with the Gator facility at LNGS. The "zero background" condition, along with a detailed knowledge of the detector geometry, allowed us to obtain a very good agreement between measured and simulated spectra, with a total uncertainty of $\sim$ 4%. In the future, we thus plan to perform a detailed validation of the GERDA Monte Carlo framework MAGE, which is a necessary step for the development of a reliable background model used in the $2\nu\beta\beta$ and $0\nu\beta\beta$ decay analyses.

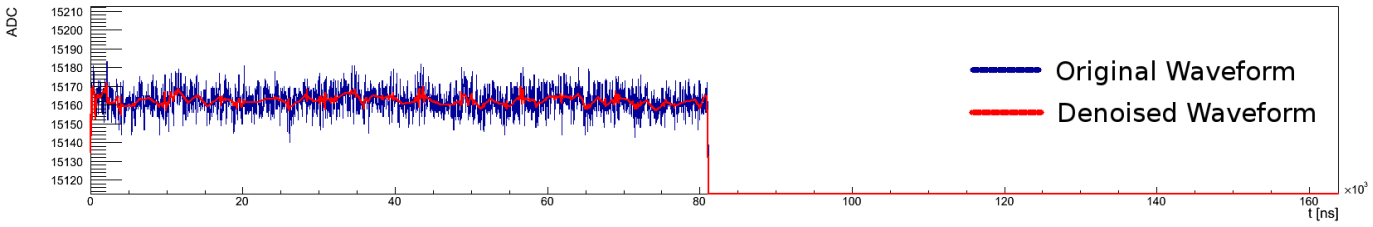

FIG. 3.6 – Wavelet trace in GERDA: baseline before and after noise reduction.

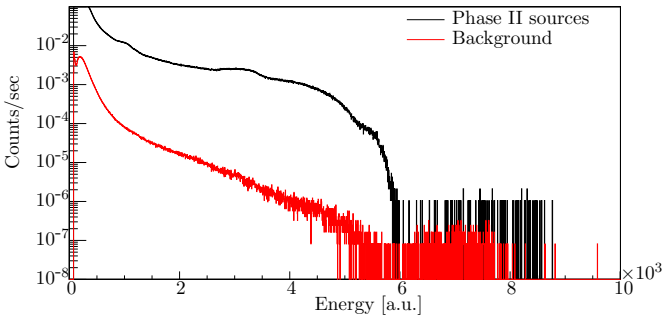

FIG. 3.7 – Energy sprectra of the LiI(Eu) detector at LNGS with/without the four GERDA Phase II ^{228}Th sources. While the γ contribution shows an endpoint at $\sim$ 6000, a thermal neutron signal is present around channel 8000. The faint peak in the background spectrum around channel 7000 might be due to an α contamination of the crystal.

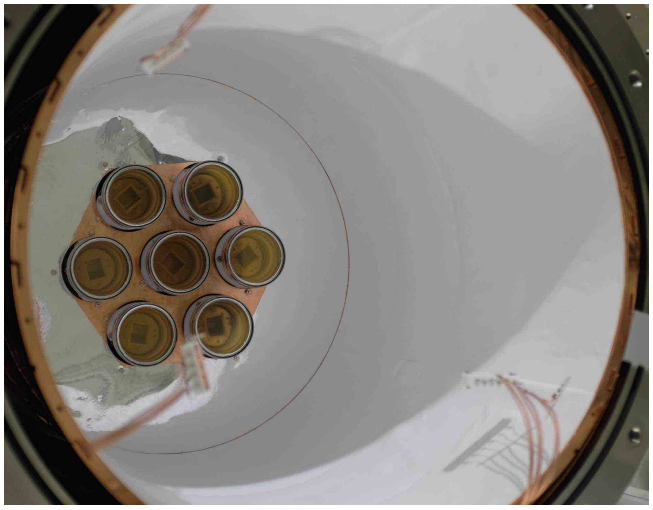

FIG. 3.8 – Bottom part of the liquid Ar veto system in GERDA, with installed Tetratex coated with TPB and the 3-inch PMT array.

3.4 The liquid argon veto

As mentioned already, in phase II the background level is to be reduced by one order of magnitude compared to phase I. Some sources of background deposit energy in the LAr surrounding the Ge detectors. The LAr instrumentation system was installed in the GERDA cryostat in early 2015. It uses two arrays of low-radioactivity Hamamatsu R11065 PMTs and SiPMs coupled to an optical fibre curtain for the light readout. Since the PMTs have a quartz window absorbing the 128 nm scintillation light and the optical fibers are not sensitive to this wavelength either, foils with wavelength shifting coatings surround the LAr.

We have produced and tested several wavelength shifting reflector foils, and Tetratex dip-coated with $\sim$0.8 mg TPB/cm^2 showed the optimal performance [11]. We then produced ten 46 cm$\times$64 cm sheets of TPB coated Tetratex and installed them in Gerda. The Tetratex foil was stitched to the copper cylinders with nylon wire. This method introduces a minimal amount of additional material and thus radioactive contamination. The completed bottom cylinder with installed PMTs is shown in Fig. 3.8.

With our LAr chamber at UZH, built for the WLS work, we will test a new version of the R11065 PMT which has a MgF_2 window. Since MgF_2 transmits 128 nm light, these PMTs could obviate the use of WLS, potentially increasing the veto signal and thus reducing the energy threshold.

[1] M. Gonzalez-Garcia, Phys. Dark Univ. 4 (2014) 1–5.

[2] S. Bilenky, C. Giunti, Int. J. Mod. Phys. A30 (2015) 0001.

[3] M. Agostini *et al.*, GERDA Collaboration, Phys. Rev. Lett. 111 (2013) 122503.

[4] K. Ackermann *et al.*, GERDA Collaboration, Eur. Phys. J. C73 (year?) page?

[5] M. Agostini *et al.*, GERDA Collaboration, Eur. Phys. J. C74 (2014) 2764.

[6] H. Klapdor-Kleingrothaus, I. Krivosheina, A. Dietz, O. Chkvorets, Phys. Lett. B586 (2004) 198–212.

[7] M. Agostini *et al.*, GERDA Collaboration, *Results on $\beta\beta$ decay with emission of two neutrinos or Majorons in ^{76}Ge from GERDA Phase I*, http://arxiv.org/abs/1501.02345

[8] M. Agostini *et al.*, GERDA Collaboration, Eur. Phys. J. C75 (2015).

[9] M. Agostini *et al.*, GERDA Collaboration, *Improvement of the Energy Resolution via an Optimized Digital Signal Processing in GERDA Phase I*, , http://arxiv.org/abs/1502.04392

[10] L. Baudis, A. Ferella, F. Froborg, M. Tarka, Nucl. Instrum. Meth. A729 (2013) 557–564.

[11] L. Baudis, G. Benato, R. Dressler, F. Piastra, I. Usoltsev *et al.*, *Fluorescence Efficiency and Stability of Radio-Pure Tetraphenyl-butadiene Based Coatings for VUV Light Detection in Cryogenic Environments*, http://arxiv.org/abs/1503.05349